EurJIC
European Journal of Inorganic Chemistry

A Journal of ChemPubSoc Europe

Accepted Article

Title: Employing linear tridentate ligands with pyrazole endgroups in catalytic tyrosinase model chemistry: Does hemilability matter?

Authors: Benjamin Herzigkeit, Ramona Jurgeleit, Benedikt Maria Flöser, Nadja Eileen Meißner, Tobias Adrian Engesser, Christian Näther, and Felix Tuczek

To be cited as: *Eur. J. Inorg. Chem.* 10.1002/ejic.201900242

Link to VoR: http://dx.doi.org/10.1002/ejic.201900242

WILEY-VCH

WILEY-VCH

FULL PAPER

Employing linear tridentate ligands with pyrazole endgroups in catalytic tyrosinase model chemistry: Does hemilability matter?

Benjamin Herzigkeit,[a] Ramona Jurgeleit,[a] Benedikt M. Flöser,[a] Nadja E. Meißner,[a] Tobias A. Engesser,[a] Christian Näther,[a] Felix Tuczek*[a]

Abstract: Several copper(I) and copper(II) complexes supported by hemilabile bis(pyrazolylmethyl)amine (**pzma**) ligands are synthesized and structurally characterized. The Cu(I) complexes with hexafluoridophosphate or perchlorate anions are employed as catalysts for the tyrosinase-like oxygenation of 2,4-di-*tert*-butylphenol (DTBP-H). Their activities are comparable to that of $[Cu(MeCN)_2$**PMP**$]PF_6$ **(PMP**= pyridylmethylpyrazol) investigated earlier. In contrast to the Cu(I) **pzma** complexes, their congeners supported by non-hemilabile bis(pyrazolylethyl)amine (**pzea**) ligands are found to be catalytically inactive.

Introduction

Copper enzymes are involved in important biochemical processes in animals or plants such as dioxygen transport and metabolism or electron transfer.[1-3] The binuclear type 3 copper enzyme tyrosinase, e.g., catalyzes the conversion of L-tyrosine to L-dopa-quinone which in turn polymerizes to melanin.[4,5] This pigment is found in plants, fungi, bacteria and mammals[6], playing key roles in skin protection against UV radiation[7], coloring of skin, hair and eyes,[8] or wound healing.[9] In 2006, Matoba *et al.* reported a crystal structure of the tyrosinase from *S. castaneoglobisporus*, providing evidence for the side-on bridging (μ-η^2:η^2) peroxo dicopper(II) core as the active species in tyrosinase-mediated oxygenation reactions.[10] Other type 3 copper proteins like catechol oxidase or hemocyanin differ in reactivity but contain similar active sites, in which each copper is coordinated by three histidines. In the meantime, more crystal structures of type 3 copper proteins have been reported, allowing to establish definite structure-function correlations in this class of enzymes.[11-13]

Artificial model systems mimicking the reactivities of type 3 copper enzymes have greatly helped elucidating the molecular mechanisms of these systems.[14,15] The first model system that is able to catalytically convert monophenols to quinones in a tyrosinase-like fashion was the binuclear copper(I) complex $[Cu_2(MeCN)_4$**BiPh(impy)$_2$**$](PF_6)_2$ by Réglier *et al.*[16]. Subsequent catalytic systems (Scheme 1) devised by Casella *et al.*[17], Stack *et al.*[18], Ottenwaelder and Lumb *et al.*[19], Herres-Pawlis *et al.*[20] and others gave rise to new functionalities and provided further mechanistic insight into details of copper-dioxygen chemistry.[21,22] So far our group exclusively used bidentate ligands like, e.g., $\mathbf{L_{py}1}$, to emulate the reactivity of tyrosinase (Scheme 1).[23] Variation of the *N* donor groups, their spatial separation and the type of counter ions was found to alter the reactivity of derived copper(I) complexes regarding the mono-oxygenation of monophenols.[23, 24, 25] In contrast to an inactive system that only contains pyridines (**DPM**), introduction of one pyrazole donor (**PMP**) or two pyrazole donors (**BPM**) increases the catalytic activity significantly.[26,27]

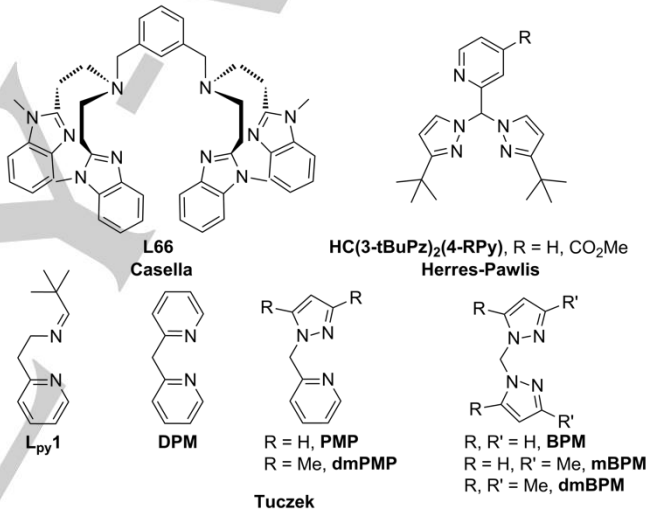

Scheme 1. Ligands used for model systems capable of oxygenation (except **DPM)** of several substrates in a tyrosinase-like reaction.[17, 20, 23-27]

In spite of the now well-established catalytic mono-oxygenation activity of copper complexes supported by simple bidentate ligands, detection of the central μ-η^2:η^2 peroxo copper(II) species has (with one exception)[18,19] always been difficult. In search of new catalytic tyrosinase models forming the seemingly elusive μ-η^2:η^2-peroxo intermediate in higher concentrations than observed so far,[27] we decided to explore threefold coordination environments which tend to better stabilize copper-dioxygen intermediates. However, with exception of the **HC(3-tBuPz)$_2$(Py)** system reported by Herres-Pawlis *et al.* and the **L66**-system of Casella *et al.* (Scheme 1),[17, 20, 21] no catalytic monooxygenation activity has been observed with such systems so far. This might be attributed to the fact that coordination of the substrate to the μ-η^2:η^2 peroxo complex, which leads to the formation of a "ternary intermediate",[15] is more difficult if each copper center is coordinated by three instead of two terminal ligands. Nevertheless, as also the example of the natural enzyme shows,[2,15] there is no reason that a threefold coordination of Cu(II) should principally preclude a catalytic monooxygenation activity of dinuclear copper sites.

[a] Benjamin Herzigkeit, Ramona Jurgeleit, Benedikt M. Flöser, Nadja E. Meißner, Dr. Tobias A. Engesser, Prof. Dr. Christian Näther, Prof. Dr. Felix Tuczek, Institut für Anorganische Chemie, Christian-Albrechts-Universität zu Kiel, Max-Eyth-Straße 2, 24118 Kiel, Germany, E-mail: ftuczek@ac.uni-kiel.de, http://www.ac.uni-kiel.de/tuczek

Supporting information for this article is given via a link at the end of the document.

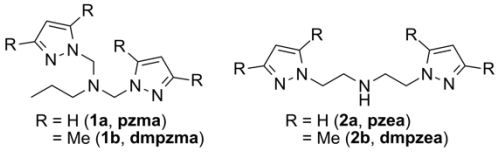

Scheme 2. Bis(pyrazolylmethyl)amine (**pzma**) ligands **1a** and **1b** and bis(pyrazolylethyl)amine (**pzea**) ligands **2a** and **2b** used in this study.

In order to obtain more information on this issue, we herein explore the use of tridentate ligands with pyrazole *N* donors (which have shown their favorable properties before; see above) in catalytic tyrosinase model chemistry. The easily accessible *N*,*N*-bis((1*H*-pyrazol-1-yl)methyl)propan-1-amine (**pzma**) ligand (Scheme 2) exhibits a central amine position which could also be used to connect two tridentate units for the synthesis of binucleating ligands. Interestingly, prior investigation of bis(pyrazolylmethyl)phenylamine ligands had evidenced hemilabile properties;[28, 29] i.e., a κ^2 coordination mode for copper(I) resembling our bidentate, catalytically active model systems and a κ^3 mode for copper(II) which should, e.g., stabilize copper(II) μ-η^2:η^2 peroxo complexes. In this context, hemilabile ligands may be useful to create a flexible coordination environment which could facilitate the coordination of external substrates for their catalytic conversion.[30] From this perspective, it appeared essential to obtain information on the coordination behavior of our ligands towards copper(I) and copper(II) centers. We thus synthesized Cu(I) and Cu(II) complexes with the new bis(pyrazolylmethyl)propaneamine (**1a**, **pzma**) and the known bis(3,5-dimethylpyrazolylmethyl)propaneamine (**1b**, **dmpzma**) ligands, which were then investigated by single-crystal X-ray structure analysis. The obtained copper(I) complexes were also employed as catalysts for the monooxygenation of the monophenol DTBP-H and the influence of different counter ions (hexafluoridophosphate and perchlorate) on the catalytic activity was studied. Finally, the effect of an elongation of the methylene groups between the pyrazole donors and the tertiary amine to ethylene bridges was examined. To this end the two known ligands bis(2-(1*H*-pyrazol-1-yl)ethyl)amine (**2a**, **pzea**) and bis(2-(3,5-dimethyl-1*H*-pyrazol-1-yl)ethyl)amine (**2b**, **dmpzea**, Scheme 2) were used for the synthesis of copper(I) complexes which were subsequently studied regarding their monophenolase activity towards DTBP-H and the formation of μ-η^2:η^2 peroxo copper(II) complexes.[31] The implications of the results regarding structure-function correlations of catalytic tyrosinase models are discussed.

Results and Discussion

Synthesis of the ligands pzma and dmpzma

The two ligands **pzma** (**1a**) and **dmpzma** (**1b**) were successfully synthesized following a procedure by Malek *et al*. (Scheme 3).[32] For the unknown compound **1a** it was necessary to prepare the alcohol **3a** in accordance with Lee *et al.* as this compound was not commercially available like **3b**.[33] By condensation of the

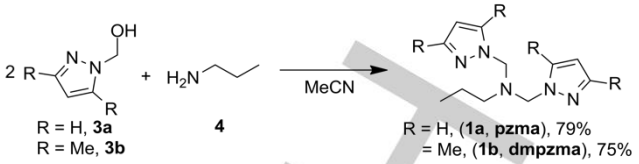

Scheme 3. Syntheses of the ligands (**pzma**, **1a** and **dmpzma**, **1b**).

alcohol **3a** or **3b** with the primary *n*-propylamine (**4**) both ligands could be obtained in good yields.[31-34]

Coordination to copper(II)

As the bipyrazolic ligands can either bind in a κ^2 or κ^3 fashion to copper centers (see above),[28,29,35] **1a** and **1b** were reacted with copper(II) perchlorate hexahydrate and copper(II) chloride dihydrate in order to determine the bonding mode to Cu(II). From these reactions six copper(II) complexes were obtained which were investigated by single-crystal X-ray diffraction (Scheme 4, Table S1).

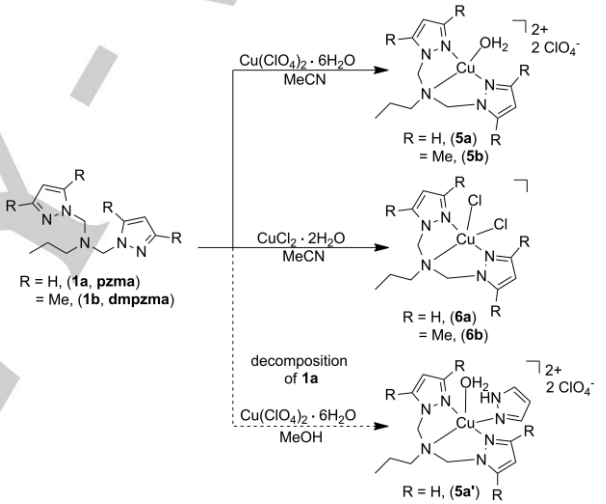

Scheme 4. Reactions of the copper precursors $Cu(ClO_4)_2 \cdot 6H_2O$ and $CuCl_2 \cdot 2H_2O$ with the ligands **1a**/**1b** to perchlorate salt **5a**/**5b** and chloride salt **6a**/**6b** as well as the decomposition reaction with methanol to form **5a'**.

Reaction of the ligands **1a** and **1b** with $Cu(II)(ClO_4)_2 \cdot 6H_2O$ in acetonitrile led to crystals showing Cu(II) cations that are 5-fold coordinated by the three N atoms of **pzma** in compound **5a** and **dmpzma** in **5b** as well as O atoms either from water molecules or from perchlorate counter ions (Figure 1). Both structures show a strongly distorted square-pyramidal geometry with water molecules in the fourth equatorial position and a water molecule (**5a**) or an anion (**5b**) in the axial position. Moreover, both structures include one O atom of a perchlorate anion at a longer distance (2.608 Å for **5a**, 2.612 Å for **5b**) which expands the coordination sphere to a strongly distorted octahedral geometry.

Using methanol as solvent led to the formation of a copper(II) perchlorate complex **5a'** in which the metal center is surrounded by one κ^3 bonded ligand **pzma** ligand, one water molecule and a 1*H*-pyrazole in a square-pyramidal geometry (Figure S2, Table S1). Presumably, the use of a protic solvent led to the decomposition of the **pzma** ligand, as already observed for similar ligands by Blackman *et al.*,[36] generating free 1*H*-pyrazole.

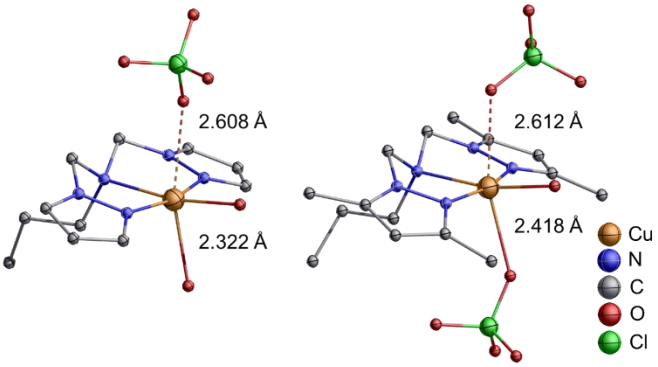

Figure 1. Crystal structure of $[Cu(H_2O)_2(\mathbf{pzma})](ClO_4)_2$ (**5a**, left) and $[Cu(H_2O)(\mathbf{dmpzma})](ClO_4)_2$ (**5b**, right). Hydrogen atoms and ClO_4 anions, that are not coordinated to the Cu center, are omitted for clarity.

Changing the reactant to copper(II) chloride led to the formation of compounds **6a** and **6b**, in which the metal ions are 5-fold coordinated by the N atoms of the κ^3 bonded **pzma**/**dmpzma** ligands and two chlorido ligands. Interestingly, in both compounds a slightly distorted trigonal bipyramidal and a square-pyramidal geometry are observed. The crystal structure of the **pzma** compound contains two crystallographically independent complexes one of which shows a trigonal-bipyramidal, the other one a square pyramidal coordination (Figure 2, a) and b)). The **dmpzma** compound, on the other hand, crystallizes in two polymorphic modifications (**6b** and **6b'**) each of which only contains one of these geometries (Figure 2, c) and d)). Taking a closer look at the structures one can see that for both ligands the axial chloride ions in the square-pyramidal structures exhibit

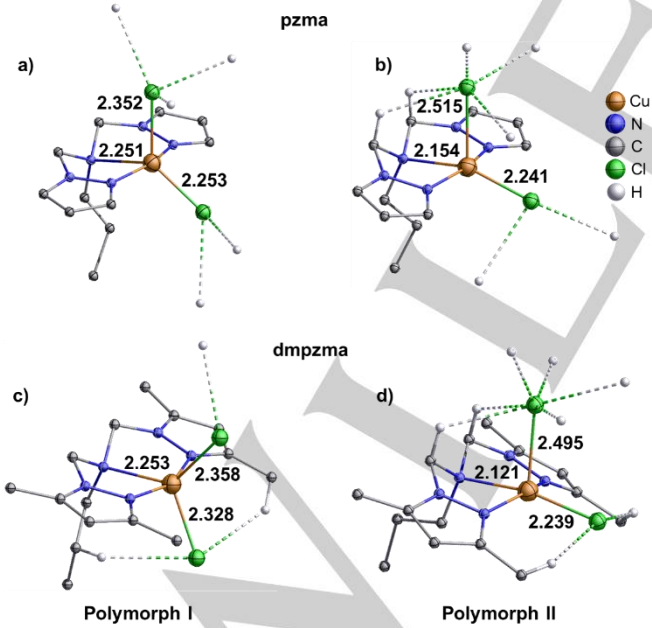

Figure 2. Molecular structures of the two crystallographically independent molecules in $[Cu(\mathbf{pzma})Cl_2]$ (**6a**, a) and b)) and in the two polymorphic modifications of $[Cu(\mathbf{dmpzma})Cl_2]$ (**6b**, c) and **6b'** d)). Only the H atoms involved in intermolecular hydrogen bonding are shown and the H-bonding is shown as dashed lines for clarity.

stronger hydrogen bonds than their counterparts within the trigonal-bipyramidal coordination. This indicates that small differences in the crystallographic environment determine the complex geometry, which in turn affects the bond lengths from the Cu(II) ion to the central amine donor (2.251 Å vs 2.154 Å (**pzma**) and 2.253 Å vs. 2.121 Å (**dmpzma**)). These structural differences indicate a very flexible (and thus potentially dissociable) bond between the Cu(II) center and the central N atom, reflecting hemilabile coordination properties of these ligands.

Coordination to copper(I)

To obtain information of the coordination behavior of ligands **1a** and **1b** to Cu(I) cations several complexes with $[PF_6]^-$ or $[ClO_4]^-$ counter anions were synthesized and structurally characterized. Specifically, the two ligands were reacted with tetrakis(acetonitrile)copper(I) hexafluoridophosphate in dichloromethane and tetrakis(acetonitrile)copper(I) perchlorate in acetonitrile in a ratio of 1:1 under anaerobic conditions to form the corresponding mono-ligated complexes (Scheme 5).

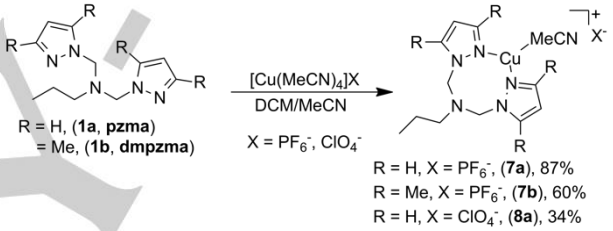

Scheme 5. Syntheses of the copper(I) complexes **7a**, **7b** and **8a**.

In case of ligand **1a**, the crystal structure of the colorless heteroleptic copper(I) complex **7a** (Figure 3, top, Table S2) could be determined. The copper(I) cation is coordinated by the ligand in a κ^2 bonding mode through the two pyrazole *N* donors and by two acetonitrile molecules. The complex exhibits a slightly

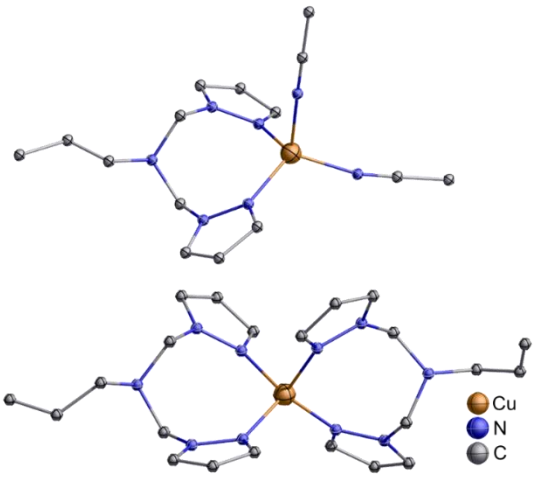

Figure 3. Crystal structure of $[Cu(MeCN)_2(\mathbf{pzma})]PF_6$ (**7a**, top) and $[Cu(\mathbf{pzma})_2]ClO_4$ (**8a'**, bottom). Hydrogen atoms, PF_6 and ClO_4 anions are omitted for clarity.

distorted tetrahedral geometry. In agreement with the hemilabile properties of the ligand the tertiary amine is not coordinated to the central copper ion in these complexes.

From the reaction of **pzma** with the Cu(I) perchlorate salt in acetonitrile small crystals of the homoleptic complex **8a'** could be obtained (Figure 3, bottom). Even though the elemental analysis of the powder is in agreement with a copper cation ligated by **1a** and two acetonitrile molecules, the crystals contain the homoleptic complex **8a'**. The same phenomenon has already been observed in our investigation of copper(I) complexes supported by the bidentate **PMP** ligand.[26] Again, the copper(I) cation is 4-fold coordinated in a slightly distorted tetrahedral geometry (Table S2).

To conclude, both Cu(I) complexes of the **pzma** ligand **1a** show a κ^2 bonding mode, similar to previously investigated Cu(I) complexes supported by bidentate ligands;[23-27] i.e., the pyrazole *N* donors are bound to the Cu(I) ion whereas the tertiary amine does not coordinate. Unfortunately, we do not have structural information on a Cu(I) complex supported by **1b**. From the fact that the ^{1}H-NMR shift of the CH_2 protons is almost unaffected by complexation (as for **1a**), we conclude that this ligand also coordinates in a κ^2 (and not in a κ^3) fashion to Cu(I).

Catalytic tyrosinase reactivity of copper(I) complexes

To investigate the catalytic activity of the heteroleptic copper(I) complexes **7a**, **7b** and **8a** oxygenation reactions were performed with DTBP-H as the substrate (Scheme 6). Upon oxygenation DTBP-H forms the highly stable *ortho*-quinone DTBQ as well as the C–C coupling byproduct 3,3',5,5'-tetra-*tert*-butyl-2,2'-biphenol (CCcP).

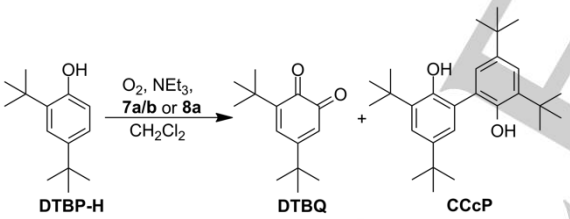

Scheme 6. Catalytic reaction of the phenolic substrate DTBP-H to *ortho*-quinone DTBQ and the byproduct CCcP.

All reactions were performed under Bulkowski/Réglier conditions.[16,37] To this end a 500 μM solution of the catalyst in dichloromethane, with 50 equivalents of substrate and 100 equivalents of triethylamine added as a base, was prepared under anaerobic conditions. Then a stream of oxygen was passed through the solution at room temperature. The generation of *ortho*-quinone was detected by *in situ* UV/vis spectroscopy through the evolution of the absorption band of DTBQ at 407 nm (ε = 1830 L mol^{-1} cm^{-1}). As shown in Table 1, the three copper(I)

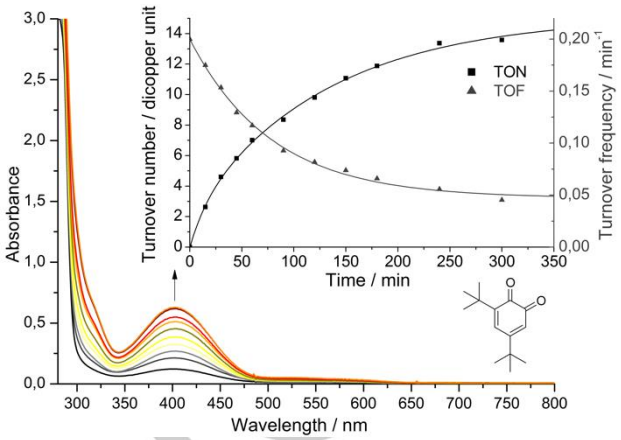

Figure 4. UV/vis spectra measured during the catalytic oxygenation of a 500 μM solution of [Cu(MeCN)**pzma**]PF_6 (**7a**) in dichloromethane in the presence of DTBP-H (50 equiv.) and triethylamine (100 equiv.) during the first 5 h at room temperature; quartz cell length l = 1 mm; inset: turnover number per dicopper unit (black squares) and turnover frequency per minute (gray triangles) as a function of time.

catalysts **7a**, **7b** and **8a** are catalytically competent towards the substrate DTBP-H. For the oxygenation of DTBP-H with **7a** a turnover number (TON) per dicopper unit of 14 was determined after 5 h (Figure 4). For catalyst **7b** a TON of 7 was reached after 5 h (Figure S20); for **8a** a TON of 15 was achieved after 6 h (Figure S21).

After the initial measurement at 15 min the TOF gradually decreases, and the reaction comes to a complete halt after 5 h for all catalysts (insets Figure S20, S21). In order to identify the reaction products a small amount of the reaction mixture was removed after 1 h, diluted to 100 μM and quenched with a 6 M hydrochloric acid. After work-up of the organic phase and removal of solvent ^{1}H and ^{13}C-NMR spectra were recorded (Figure S22-S27). According to the ^{1}H-NMR spectrum the ratio of DTBP-H, DTBQ and CCcP for **7a** was 90 % DTBP-H, 6 % DTBQ and 4 % CCcP, which corresponds to the TON of 7 detected by UV/vis spectroscopy after 1 h. For **7b** a ratio of 91 % DTBP-H, 4 % DTBQ and 5 % CCcP and for **8a** 84 % DTBP-H, 8 % DTBQ and 8 % CCcP after 1 h was determined (Figure S22-S27, Table S11).

The TONs achieved by our new catalytic model systems **7a**, **7b** and **8a** are collected in Table 1 and compared with those reached by our previously investigated systems.[23, 26] With different anions (PF_6^- or ClO_4^-) only marginal differences of the TONs are observed. Sterically more encumbered, methylated **7b** exhibits a lower TON for DTBP-H as its parent congener. In comparison with older model systems the new catalysts can be ranked in a similar category as the **PMP** systems.[26] With **7a** (TON = 14) and **8a** (15), catalytic activity towards DTBP is nearly equal to the **PMP** system (14), but lower than for the symmetric

Table 1. Overview of the tyrosinase-like activity (TON) for the conversion of DTBP-H, mediated by the new systems (shaded) and systems supported by bidentate ligands

Systems	**DPM** [23]	**BPM** [27]	**dmBPM** [27]	**PMP** [26]	**dmPMP** [26]	**7a** ***this work***	**7b** **this work**	**8a** ***this work***
DTBP-H	0	21	11	14	11	14	7	15

BPM system (21). The same applies to methyl substituted **7b** (7) if compared with its **dmPMP** (11) or **dmBPM** (11) counterparts.

Increasing the alkyl spacer length: pzea ligands

The mechanistic cycle associated with the new copper(I) complexes **7a**, **7b** and **8a** can be assumed to be similar to that of previously published catalytic tyrosinase model systems.[15,19,20,23] Initially, we thought that a tridentate ligand design might favor the formation of the central μ-η^2:η^2 peroxo adduct as a key intermediate (see above); however, in spite of numerous attempts (Table S12) we were unable to detect this species. We speculated that that the five-ring metallacycles obtained upon coordination of **pzma** to copper(II) (see above) might eventually be unfavorable for the stabilization of the μ-η^2:η^2 peroxo dicopper core. Although examples of μ-η^2:η^2 peroxo dicopper complexes supported by *NNN*-type ligands with five-ring metallacycles exist[14, 38], we note that Casella´s **L-66** complex exhibiting six-ring metallacycles forms a μ-η^2:η^2 peroxo intermediate[17b] whereas its **L-55** counterpart exhibiting five-ring metallacycles does not.[39] To check whether elongation of the methylene to ethylene bridges in the **pzea** ligands would increase the stability of the side-on peroxo dicopper complex, we synthesized the tridentate bis(pyrazolyl-ethyl)amine ligands **2a** and **2b** after a procedure of Blackman *et al.* and Khlebnikov *et al*.[31, 36] Apart from the length of the bridges, these ligands also differ from **1a** and **1b** by the presence of a secondary instead of a tertiary amine group at the central position.

Using one equivalent of ligands **2a**/**2b** and one equivalent of $[Cu(MeCN)_4]PF_6$, the mono-ligated κ^3 coordinated copper(I) complexes **9a**/**9b** could be prepared (Scheme 7). Sorrell *et al.* were able to obtain a crystal structure of **2b** with a copper(I) $[BF_4]^-$-salt confirming the κ^3 coordination mode even for the copper(I) complexes, in contrast to the **pzma** systems.[40] This suggests the absence of hemilabile properties for the **pzea**-type ligands **2a**/**2b**, which is also corroborated by the fact that the coexistence of trigonal-biypramidal and square-planar coordination geometries observed for Cu(II) complexes of **pzma** ligands (see above) is not found for corresponding **pzea** complexes. As a matter of fact, these complexes exclusively exhibit square-pyramidal geometries, implying a central amine donor that is strongly bound to the metal center.[36]

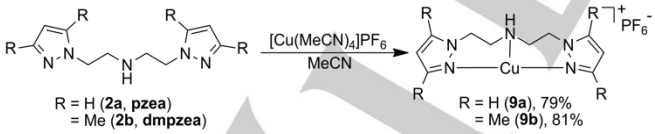

Scheme 7. Syntheses of the copper(I) complexes **9a**/**9b**.

To investigate the oxygenation behavior of **9b** low temperature UV/vis spectroscopy was employed (Figure 5). The 3,5-dimethylpyrazol-substituted variant of the ligand was used as it should shield the peroxo core better than its unsubstituted analog and thus increase its thermal stability. Indeed, we were able to observe the formation of an absorption band at 353 nm which can be assigned to the in-plane $\pi_{\sigma^*} \rightarrow d_{x^2-y^2}$ transition of the Cu_2O_2-core (cf TD-DFT in Figure S32).[14,15] Based on an ε value

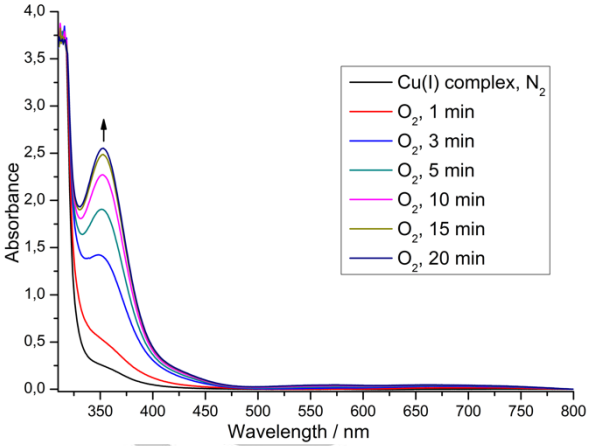

Figure 5. Low temperature UV/vis spectra measured during the generation of the μ-η^2:η^2 peroxo copper(II) complex from **9b** in acetone at -90 °C; quartz cell length l = 1cm.

of 20.000 L mol^{-1} cm^{-1} for the 353 nm band the yield of the peroxo complex is estimated to 12.5 %.[41]

Subsequently the reactivity of the copper(I) complexes **9a** and **9b** towards DTBP-H was investigated, and an almost vanishing TON of 2 was obtained under Bulkowski/Réglier conditions for both systems (Figure S33-S34). Thus, although the copper(I)-**pzea** complexes **9a** and **9b** are much more prone towards formation of the side-on peroxo dicopper intermediate than their **pzma** congeners, they are catalytically almost inactive, in contrast to the latter. This indicates once again that a stable side-on peroxo intermediate does not necessarily go along with a catalytic activity for a small-molecule model of tyrosinase or, conversely, that catalytically active model systems often do not allow detecting the characteristic peroxo intermediate. Nevertheless, due to their low reactivity, copper **pzea** complexes might be useful in future studies to elucidate the mechanism of the monooxygenation reaction in a stoichiometric mode.[23a] Moreover, by using the central amine function to connect two tridentate units, dinucleating ligands could be synthesized which might result in copper complexes that stabilize the peroxo core even more.

Conclusions

Five new copper(I) complexes and six new copper(II) complexes supported by bis(pyrazolylmethyl)amine (**pzma)** ligands were prepared. These ligands exhibit hemilabile properties; i.e., they bind in a κ^2 fashion through the two N_{pz} donors to copper(I) and in a κ^3 bonding mode to copper(II). The copper(I) **pzma** complexes act as catalysts in a tyrosinase-like monooxygenation of the phenol DTBP-H. TONs for the new complexes (14-15) can be ranked in the same category as the earlier investigated **PMP** systems (14) regarding this substrate. Again, the use of pyrazoles as *N* donors turned out to be favorable for an increased catalytic activity of copper-based tyrosinase models. Based on copper complexes supported by the new tridentate **pzma** ligands, we expected a better stabilization of the corresponding μ-η^2:η^2 peroxo dicopper(II) intermediates in comparison to systems

supported by simple bidentate ligands employed earlier. However, we were again unable to detect these species. On the other hand, using a Cu(I) complex supported by the analogous bis(pyrazolylethyl)amine (**dmpzea**) ligand with ethyl bridges between the *N* donors of the ligand did allow detection of the μ-η^2:η^2 peroxo-complex. Nevertheless, both Cu(I) **pzea** complexes were found to be almost inactive (TON = 2) regarding the catalytic monooxygenation of DTBP-H. These differences may be attributed to the fact that **pzma** ligands are hemilabile whereas **pzea** ligands are not. This would indicate that hemilability of supporting tridentate ligands is important in tyrosinase model chemistry to enable formation of the ternary intermediate which involves simultaneous binding of dioxygen and the substrate to the metal centers. Further examination of this hypothesis is under way.

Experimental Section

Materials and Methods

Chemicals and solvents were purchased from Sigma-Aldrich Co. LLC, Deutero and Fisher Scientific in reagent grade. Dichloromethane and acetonitrile were further purified by heating to reflux over calcium hydride and distilled under a nitrogen atmosphere. Acetone was further purified by heating over Drierite™ and distilled under a nitrogen atmosphere. Synthesis of the copper(I) complexes and preparation of the oxygenation mixtures were performed in a glovebox (MBraun, O_2 < 1 ppm; H_2O < 1 ppm). Flash column chromatography was carried out by using an Isolera One spectra system by co. Biotage with an UV detector (200-400 nm) and prepacked SNAP Ultra cartridges (25 g). Rf-values were determined by thin-layer chromatography on Polygram Sil G/UV254 (Macherey-Nagel, 0.2 mm particle size) with a UV lamp (λ = 254 nm) by co. Camag. NMR spectra were recorded at 300 K using a Bruker DRX 500 [^{1}H NMR (500.1 MHz), ^{13}C NMR (125.8 MHz)] and a Bruker AVANCE III HD Pulse Fourier Transform spectrometer operating at frequencies of 400.13 MHz (^{1}H), 100.62 MHz (^{13}C) with TMS as internal standard. The elemental analyses were performed using a vario MICRO cube element analyzer by co. Elementar: The prepared assays in tin vessels were burnt in a stream of oxygen. Infrared spectra were recorded on a Bruker ALPHA FT-IR Spectrum with a Platinum ATR setup. UV/vis measurements of the oxygenation mixtures were recorded in solution on an Agilent 8453 spectrometer by using a quartz cell with length l = 1 mm. Optical absorption spectra at low temperatures were recorded in solution on an Agilent Cary 5000 spectral photometer using a CryoVAC KONTI cryostat with a quartz cell length l = 1 cm.

Single-crystal structure determinations

Data collections were performed with an imaging plate diffraction system IPDS-2 from STOE & CIE using Mo-Kα-radiation. The data were corrected for absorption using programs X-RED and X-SHAPE of the program package X-Area. The structure solution was performed with SHELXT and structure refinement was done against F^2 using SHELXL-2014. All non-hydrogen atoms, except of some which are disordered. were refined anisotropic, The C-H H atoms were positioned with idealized geometries (methyl H atoms allowed to rotate but not to tip) and were refined isotropic with U_{iso}(H) = -1.2 U_{eq}(C) (1.5 for methyl H atoms) using a riding model. In **5a** and **5a'** and **5b** the O-H H atoms were located in difference map, their bond lengths were set to ideal values and finally they were refined isotropic with U_{iso}(H) = 1.5 U_{eq}(O) using a riding model in **7a** and **8a'** one of the propyl group as well as the hexafluoridophosphate respectively perchlorate anion are disordered in two orientations and were refined using a split model with restraints (SAME/SIMU/DELU). Disorder of the perchlorate anions is also observed in **5a** and **5a'** where restraints for the bond lengths (SAME) were used. In **6a** one of the propyl groups is disordered and was refined using a split model with restraints and the C atoms of lower occupancy were refined only isotopic. After structure refinement of **6b**, there is one significant residual electron density peak close to the copper and one N atom, which might be traced back to the fact that some twinning is observed that cannot be modeled. The crystal of **6b'** was non-merohedral twinned and therefore, a twin refinement was performed using data in HKLF-5 format. In this case symmetry equivalent reflections were merged and no reasonable absorption correction can be performed. For **8a'** the absolute structure was determined and is in agreement with the selected setting (Flack x-parameter: -0.006(4)). CCDC-1896656 (**5a**), CCDC-1896654 (**5a'**), CCDC-1896657 (**5b**), CCDC-1896655 (**6a**), CCDC-1896652 (**6b**), CCDC-1896653 (**6b'**), CCDC-1896651 (**7a**) and CCDC-1896658 (**8a'**), contain the supplementary crystallographic data for this paper. These data can be obtained free charge from the Cambridge Crystallographic Data Centre via http://www.ccdc.cam.ac.uk/data_request/cif.

General procedure for the oxygenation and quenching of external substrates with copper(I) complexes

The copper catalyst (1.25 μmol) was dissolved in dry dichloromethane (25 mL) under an inert gas atmosphere with monophenol (50 equiv., 62.5 μmol) and triethylamine (100 equiv., 0.125 mmol) resulting in a 500 μM solution. Subsequent injection of dioxygen at ambient temperature leads to the oxygenation of monophenols to their corresponding *ortho*-quinones, identified via UV/vis spectroscopy by absorption bands at the range of 390–425 nm. For further characterization of the formed organic reaction products an aliquot (5 mL) was removed from the reaction mixture and diluted to a 100 μM solution in dichloromethane. After treatment with 6 M hydrochloric acid (20 mL) the organic phase was separated, the aqueous phase extracted with dichloromethane (2 x 20 mL), the organic phases combined, dried with magnesium sulfate, filtered, and solvents evaporated under reduced pressure. The obtained residue was analysed via ^{1}H- and ^{13}C-NMR spectroscopy (see Supporting information).

General procedure for the low temperature UV/vis measurement of 9b

For the detection of the μ-η^2:η^2 peroxo copper(II) complex of **9b** low temperature UV/vis measurements were done by cooling a 2 mM solution of complex **9b** in acetone to -90 °C under an N_2 atmosphere. After injection of O_2 formation of the copper/oxygen species could be identified via UV/vis spectroscopy by absorption bands at 353 nm and 653 nm.

Experimental Section

***N*,*N*-Bis((1*H*-pyrazol-1-yl)methyl)propan-1-amine** (**1a**, **pzma**)

1-Hydroxymethyl-pyrazole (1.96 g, 20.0 mmol) (**3a**) was dissolved in acetonitrile (10 mL) and *n*-propylamine (0.59 g, 10 mmol) (**4**) dissolved in acetonitrile (2 mL) added to the mixture. The solution was stirred under reflux for 6 h. The solvent was evaporated under reduced pressure and the oily residue was dissolved in dichloromethane (10 mL) and washed with dist. water (2 x 10 mL). The organic phases were combined, dried with sodium sulfate, filtered and the solvent evaporated under reduced pressure. The crude product was purified by column chromatography on silica gel (cyclohexane/ethyl acetate, 1:2, Rf = 0.35) to obtain the desired product as a colorless oil (1.74 g, 7.93 mmol, 79 %). IR (ATR): $\tilde{\nu}$ = 3107

(w), 2962 (m), 2933 (w), 1512 (m), 1461 (m), 1443 (m), 1392 (m), 1376 (m), 1345 (m), 1247 (m), 1227 (w), 1198 (w), 1167 (w), 1084 (s), 1045 (s), 961 (m), 879 (m), 843 (m), 747 (s), 653 (m), 616 (s), 545 (w) cm^{-1}. ^1H NMR (500 MHz, $CDCl_3$, 300 K): δ = 7.53 (dd, ^3J = 4.3, ^4J = 1.9 Hz, 4 H, C_{pz}-*H*3, C_{pz}-*H*5), 6.28 (t, 2 H, ^3J = 2.1 Hz, C_{pz}-*H*4), 5.01 (s, 4 H, N_{pz}-C*H*$_2$), 2.60 (m, 2 H, C*H*$_2$-CH$_2$-CH$_3$), 1.53 (m, 2 H, CH$_2$-C*H*$_2$-CH$_3$), 0.86 (t, ^3J = 7.4 Hz, 3 H, CH$_2$-CH$_2$-C*H*$_3$) ppm. ^{13}C NMR (126 MHz, $CDCl_3$, 300 K): δ = 139.7 (C_{pz}-3), 129.8 (C_{pz}-5), 106.0 (C_{pz}-3), 67.8 (N_{pz}-CH$_2$), 52.0 (*C*H$_2$-CH$_2$-CH$_3$), 20.8 (CH$_2$-*C*H$_2$-CH$_3$), 11.6 (CH$_2$-C*H*$_2$-*C*H$_3$) ppm. $C_{11}H_{17}N_5$ (219.3): calcd. C 60.25, H 7.81, N 31.94; found C 60.40, H 8.12, N 31.85.

[Cu(H$_2$O)(1a)](ClO$_4$)$_2$ [Cu(H$_2$O)(pz)(1a)](ClO$_4$)$_2$ (5a)

To a solution of **1a** (169 mg, 0.772 mmol) in acetonitrile (3 mL) copper(II)perchlorate hexahydrate (286 mg, 0.772 mmol) dissolved in acetonitrile (3 mL) was added dropwise. The solution was stirred for 30 min at room temperature. After layering the solution with diethyl ether a blue solid precipitated after 18 h. The precipitate was filtered, washed with diethyl ether and dried under reduced pressure to obtain a blue solid (268 mg, 0.536 mmol, 69 %). Doing the same procedure in methanol blue crystals suitable for X-ray structure determination were obtained after layering the reaction mixture with diethyl ether. The blue crystals were identified as compound **5a'**. IR (ATR): $\tilde{\nu}$ = 3356 (w, br), 3223 (w), 3135 (w), 2964 (w), 1655 (w), 1602 (w), 1520 (w), 1490 (m), 1402 (w), 1263 (m), 1212 (w), 1088 (s), 1035 (s), 992 (s), 922 (m), 790 (m), 771 (m), 618 (s), 606 (s), 581 (s) cm^{-1}. $C_{11}H_{19}Cl_2CuN_5O_9$ (499.7): calcd. C 26.44, H 3.83, N 14.01; found C 26.12, H 4.23, N 13.66.

[Cu(H$_2$O)(1b)](ClO$_4$)$_2$ (5b)

Complex **5b** was prepared in the same manner as described for **6a** using copper(II)perchlorate hexahydrate (165 mg, 0.600 mmol) and **1b** (222 mg, 0.600 mmol). The desired product was obtained as a blue solid (230 mg, 0.414 mmol, 69 %). Layering an acetonitrile solution of **6b** with diethyl ether led to crystals suitable for X-ray structure determination after 3 d. The blue crystals were identified as compound **6b**. IR (ATR): $\tilde{\nu}$ = 3323 (w, br), 3248 (w), 3137 (w), 2986 (w), 2927 (w), 2882 (w), 1633 (w), 1569 (w), 1551 (m), 1498 (w), 1471 (m), 1418 (w), 1396 (m), 1104 (s), 1051 (s), 922 (m), 859 (m), 822 (m), 749 (w), 618 (s), 577 (m) cm^{-1}. $C_{15}H_{27}Cl_2CuN_5O_9$ (555.9): calcd. C 32.41, H 4.90, N 12.60; found C 32.81, H 5.30, N 12.79.

[Cu(1a)]Cl$_2$ (6a)

Complex **6a** was prepared in the same manner as described for **6a** using copper(II)chloride dihydrate (162 mg, 0.949 mmol) and **1a** (208 mg, 0.949 mmol). The desired product was obtained as a blue solid (198 mg, 0.560 mmol, 59 %). Layering an acetonitrile solution of **6a** with diethyl ether led to crystals suitable for X-ray structure determination after 5 d. The green crystals were identified as compound **6a**. IR (ATR): $\tilde{\nu}$ = 3117 (m), 3097 (m), 3088 (m), 2974 (w), 2954 (w), 2876 (w), 1510 (w), 1467 (m), 1453 (m), 1398 (m), 1345 (w), 1263 (s), 1155 (w), 1092 (m), 1064 (s), 986 (s), 855 (m), 802 (s), 761 (s), 645 (m), 610 (m) cm^{-1}. $C_{11}H_{17}Cl_2CuN_5$ (353.7): calcd. C 37.35, H 4.84, N 19.80; found C 37.09, H 4.89, N 19.76.

[Cu(1b)]Cl$_2$ (6b)

Complex **6b** was prepared in the same manner as described for **6a** using copper(II)chloride dihydrate (75.6 mg, 0.443 mmol) and **1b** (122 mg, 0.443 mmol). The desired product was obtained as a green solid (139 mg, 0.339 mmol, 77 %). Layering an acetonitrile solution of **6b** with diethyl ether led to crystals suitable for X-ray structure determination after 1 d. The green crystals were identified as compound **6b**, which crystallizes in two polymorphic modifications (**6b** and **6b'**), of which one crystallizes as needles, the other as blocks (Figure S7). In the synthesis always mixtures of both polymorphic forms were obtained and for XRPD investigations these crystals were selected by hand (Figure S8 and S9). IR (ATR): $\tilde{\nu}$ = 3427 (m, br), 3387 (m, br), 3133 (w), 2956 (m), 2874 (m), 2090 (w), 1635 (m), 1551 (s), 1463 (m), 1418 (m), 1388 (s), 1302 (m), 1271 (s), 1133 (m), 1061 (s), 982 (m), 924 (m), 861 (m), 794 (s), 698 (w), 606 (w), 569 (s), 461 (s) cm^{-1}. $C_{15}H_{25}Cl_2CuN_5$ (409.8): calcd. C 43.96, H 6.15, N 17.09; found C 44.04, H 6.40, N 17.14.

[Cu(MeCN)(1a)]PF$_6$ (7a)

Tetrakis(acetonitrile)copper(I) hexafluoridophosphate (219 mg, 0.588 mmol) was dissolved in 4 mL dry dichloromethane and a 8 mL solution of **1a** (129 mg, 0.588 mmol) in dry dichloromethane was slowly added via a syringe. The colorless solution was stirred for 30 min at room temperature and the solvent evaporated under reduced pressure. The desired product was obtained as a colorless solid (239 mg, 0.510 mmol, 87 %). Slow evaporation of **7a** in acetonitrile led to crystals suitable for X-ray structure determination after one week. The colorless crystals were identified as **7a** with an additional acetonitrile ligand coordinated. IR (ATR): $\tilde{\nu}$ = 3152 (w), 3135 (w), 2966 (w), 2939 (w), 2876 (w), 2302 (w), 2272 (w), 1514 (w), 1435 (m), 1402 (m), 1373 (w), 1282 (w), 1245 (w), 1198 (w), 1124 (w), 1092 (m), 1057 (m), 963 (w), 828 (vs), 761 (s), 732 (s), 645 (w), 610 (m), 555 (s) cm^{-1}. ^1H NMR (400 MHz, CD_3CN, 300 K): δ = 7.74 (s, 2 H, C_{pz}-*H*3), 7.61 (s, 2H, C_{pz}-*H*5), 6.40 (s, 2 H, C_{pz}-*H*4), 5.06 (s, 4 H, N_{pz}-C*H*$_2$), 2.70–2.44 (m, 2 H, C*H*$_2$-CH$_2$-CH$_3$), 1.96 (s, 3 H, C*H*$_3$CN), 1.53 – 1.39 (m, 2 H, CH$_2$-C*H*$_2$-CH$_3$), 0.83 (t, ^3J = 7.3 Hz, 3 H, CH$_2$-CH$_2$-C*H*$_3$) ppm. ^{13}C NMR (101 MHz, CD_3CN, 300 K): δ = 141.2 (C_{pz}-3), 132.6 (C_{pz}-5), 118.3 (CH$_3$*C*N), 107.1 (C_{pz}-4), 67.9 (N_{pz}-CH$_2$), 52.5 (*C*H$_2$-CH$_2$-CH$_3$), 21.3 (CH$_2$-*C*H$_2$-CH$_3$), 11.5 (CH$_2$-C*H*$_2$-*C*H$_3$), 1.62 (CH$_3$*C*N) ppm. $C_{15}H_{23}CuF_6N_7P$ (509.9): calcd. C 35.33, H 4.30, N 19.23; found C 35.19, H 4.26, N 19.16.

[Cu(MeCN)(1b)]PF$_6$ (7b)

Complex **7b** was prepared in the same manner as described for **7a** using Tetrakis(acetonitrile)copper(I) hexafluoridophosphate (149 mg, 0.400 mmol) and **1b** (110 mg, 0.400 mmol). The desired product was obtained as a colorless solid (125 mg, 0.238 mmol, 60 %). IR (ATR): $\tilde{\nu}$ = 3135 (w), 2966 (w), 2933 (w), 2872 (w), 1553 (w), 1463 (m), 1427 (w), 1394 (m), 1302 (w), 1282 (w), 1241 (w), 1190 (w), 1082 (w), 1020 (w), 828 (vs), 753 (m), 753 (m), 692 (w), 628 (w), 555 (s) cm^{-1}. ^1H NMR (400 MHz, CD_3CN, 300 K): δ = 6.04 (s, 2 H, C_{pz}-*H*4), 4.82 (s, 4 H, N_{pz}-C*H*$_2$), 2.64–2.55 (m, 2 H, C*H*$_2$-CH$_2$-CH$_3$), 2.30 (s, 6 H, C_{pz}3-CH$_3$), 2.29 (s, 6 H, C_{pz}5-CH$_3$), 1.96 (s, 3 H, C*H*$_3$CN), 1.60 – 1.45 (m, 2 H, CH$_2$-C*H*$_2$-CH$_3$), 0.90 (t, ^3J = 7.3 Hz, 3 H, CH$_2$-CH$_2$-C*H*$_3$) ppm. ^{13}C NMR (101 MHz, CD_3CN, 300 K): δ = 150.1 (C_{pz}-3), 142.7 (C_{pz}-5), 118.3 (CH$_3$*C*N), 107.5 (C_{pz}-4), 62.9 (N_{pz}-CH$_2$), 53.3 (*C*H$_2$-CH$_2$-CH$_3$), 21.6 (CH$_2$-*C*H$_2$-CH$_3$), 14.0 (C_{pz}3-CH$_3$), 11.9 (CH$_2$-C*H*$_2$-CH$_3$), 11.6 (C_{pz}5-CH$_3$), 1.62 (CH$_3$*C*N) ppm. $C_{17}H_{28}CuF_6N_6P$ (525.0): calcd. C 38.90, H 5.38, N 16.01; found C 38.89, H 5.32, N 15.68.

[Cu(MeCN)$_2$(1a)]ClO$_4$ (8a)

Tetrakis(acetonitrile)copper(I) perchlorate (122 mg, 0.544 mmol) was dissolved in 4 mL dry acetonitrile and a 6 mL solution of **1a** (150 mg, 0.544 mmol) in dry acetonitrile was slowly added via a syringe. The colorless solution was stirred for 30 min at room temperature and the solvent evaporated under reduced pressure. The desired product was obtained as a colorless solid (90.7 mg, 0.182 mmol, 34 %). Slow evaporation of **8a** in acetonitrile led to crystals suitable for X-ray structure determination after two weeks. The colorless crystals were identified as homoleptic complex **8a'**. IR (ATR): $\tilde{\nu}$ = 3125 (w), 2966 (w), 2937 (w), 2874 (w), 2270 (w), 1518 (w), 1465 (w), 1398 (m), 1343 (w), 1280 (m), 1247 (w), 1198 (w), 1075 (vs), 977 (w), 898 (w), 832 (w), 761 (s), 732 (m), 651 (w), 618 (s), 553 (w) cm^{-1}.

^{1}H NMR (400 MHz, CD_3CN, 300 K): δ = 7.77 (s, 2 H, C_{pz}-*H*3), 7.64 (s, 2 H, C_{pz}-*H*5), 6.60-6.26 (m, 2 H, C_{pz}-*H*4), 5.07 (s, 4 H, N_{pz}-C*H*$_2$), 2.59 (s, 2 H, C*H*$_2$-CH_2-CH_3), 1.96 (s, 6 H, C*H*$_3$CN), 1.45 (dd, 2 H, ^{3}J = 13.6, 7.5 Hz, CH_2-C*H*$_2$-CH_3), 0.83 (t, ^{3}J = 7.2 Hz, 3 H, CH_2-CH_2-C*H*$_3$) ppm. ^{13}C NMR (101 MHz, CD_3CN, 300 K): δ = 141.5 (C_{pz}-3), 132.9 (C_{pz}-5), 118.3 (CH_3*C*N), 107.4 (C_{pz}-4), 67.9 (N_{pz}-CH_2), 52.5 (*C*H_2-CH_2-CH_3), 21.2 (CH_2-*C*H_2-CH_3), 11.5 (CH_2-C*H*$_2$-*C*H_3), 1.62 (CH_3*C*N) ppm. $C_{15}H_{23}ClCuN_7O_4$ (464.4): calcd. C 38.80, H 4.99, N 21.11; found C 38.84, H 4.93, N 20.85.

[Cu(2a)]PF_6 (9a)

Tetrakis(acetonitrile)copper(I) hexafluoridophosphate (194 mg, 0.521 mmol) was dissolved in 3 mL dry acetonitrile and a 5 mL solution of **2a** (107 mg, 0.521 mmol) in dry acetonitrile was slowly added via a syringe. The colorless solution was stirred for 30 min at room temperature and the solvent evaporated under reduced pressure. The desired product was obtained as a colorless solid (171 mg, 0.413 mmol, 79 %). IR (ATR): $\tilde{\nu}$ = 3315 (w), 3152 (w), 2905 (w), 2870 (w), 1519 (w), 1449 (w), 1439 (w), 1416 (m), 1380 (w), 1335 (w), 1296 (m), 1271 (w), 1208 (w), 1180 (w), 1126 (w), 1104 (w), 1073 (m), 1016 (w), 920 (w), 822 (vs), 761 (s), 643 (m), 555 (s) cm^{-1}. ^{1}H NMR (400 MHz, CD_3CN, 300 K): δ = 7.60-7.59 (m, 4 H, C_{pz}-*H*3, C_{pz}-*H*5), 6.34 (t, ^{3}J = 2.2 Hz, 2 H, C_{pz}-*H*4), 4.21-4.19 (m, 4 H, N_{pz}-C*H*$_2$-CH_2-NH), 3.00-2.97 (m, 4 H, N_{pz}-CH_2-C*H*$_2$-NH) ppm. ^{13}C NMR (101 MHz, CD_3CN, 300 K): δ = 141.0 (C_{pz}-3), 132.2 (C_{pz}-5), 106.3 (C_{pz}-4), 51.4 (N_{pz}-CH_2-CH_2), 50.8 (NH-CH_2-CH_2) ppm. $C_{10}H_{15}CuF_6N_5P$ (413.8): calcd. C 29.03, H 3.65, N 16.93; found C 29.21, H 3.73, N 16.77.

[Cu(2b)]PF_6 (9b)

Complex **9b** was prepared in the same manner as described for **9a** using Tetrakis(acetonitrile)copper(I) hexafluoridophosphate (150 mg, 0.513 mmol) and **2b** (105 mg, 0.402 mmol). The desired product was obtained as a colorless solid (153 mg, 0.326 mmol, 81 %). IR (ATR): $\tilde{\nu}$ = 3307 (w), 2933 (w), 2874 (w), 1551 (w), 1463 (m), 1437 (w), 1423 (w), 1390 (m), 1312 (w), 1231 (w), 1122 (w), 1057 (w), 1033 (w), 930 (w), 831 (vs), 741 (m), 620 (w), 555 (s) cm^{-1}. ^{1}H NMR (400 MHz, CD_3CN, 300 K): δ = 5.95 (s, 2 H, C_{pz}-*H*4), 3.95-3.97 (m, 4 H, N_{pz}-C*H*$_2$-CH_2-NH), 2.99 (s, 4 H, N_{pz}-CH_2-C*H*$_2$-NH), 2.26 (s, 6 H, C_{pz}3-C*H*$_3$), 2.22 (s, 6 H,C_{pz}5-C*H*$_3$) ppm. ^{13}C NMR (101 MHz, CD_3CN, 300 K): δ = 148.8 (C_{pz}-3), 141.8 (C_{pz}-5), 105.9 (C_{pz}-4), 50.5 (N_{pz}-*C*H_2-CH_2), 47.2 (NH-CH_2-*C*H_2), 14.2 (C_{pz}3-*C*H_3) 11.4 (C_{pz}5-*C*H_3) ppm. $C_{14}H_{23}CuF_6N_5P$ (469.9): calcd. C 35.79, H 4.93, N 14.90; found C 35.82, H 5.05, N 14.90.

Acknowledgements

The authors thank S. Pehlke and J. Pick for the spectroscopic measurements as well as I. Jeß for the measurement of the crystals and the CAU Kiel for financial support of this research.

Keywords: Tyrosinase • enzyme models• coordination modes • pyrazolic compounds • homogeneous catalysis • *N*-donor ligands

[1] a) M. E. Dirks-Hofmeister, R. Singh R, C. M. Leufken, J. K. Inlow, B. M. Moerschbacher, *PLoS One* **2014**, 9: e99759.; b) E. Buitrago, R. Hardre, R. Haudedoeur, H. Jamet, C. Belle, A. Boumendjel, L. Bubacco, M. Reglier, *Current Topics in Medicinal Chemistry* **2016**, *16*, 3033.; c) K. E. van-Holde, K. I. Miller, H. Decker, *J. Biol. Chem.* **2001**, *276*, 15563.

[2] a) H. Decker, T. Schweikardt, F. Tuczek, *Angew. Chem. Int. Ed.* **2006**, *45*, 4546–4550; *Angew. Chem.* **2006**, *118*, 4658–4663.; b) H. Claus, H. Decker, *Syst Appl Microbiol.* **2006**, *29*, 3–14.

[3] a) N. Fujieda and S. Itoh, *Chem. Soc. Jpn.* **2016**, *89*, 733.; b) N. Fujieda, M. Murata, S. Yabuta, T. Ikeda, C. Shimokawa, Y. Nakamura, Y. Hata and S. Itoh, *J. Biol. Inorg. Chem.* **2013**, *18*, 19.; c) S. Itoh, H. Kumei, M. Taki, S. Nagatomo, T. Kitagawa, S. Fukuzumi, *J. Am. Chem. Soc.* **2001**, *123*, 6708.

[4] a) J.-S. Taylor, *Science* **2015**, *347*, 824; b) C. Olivares, F. Solano, *Pigment Cell Melanoma Res.* **2009**, *22*, 750; c) E. Dadachova, R. A. Bryan, X. Huang, T. Moadel, A. D. Schweitzer, P. Aisen, J. D. Nosanchuk, A. Casadevall, *PLoS ONE* **2007**, *2*, e457.

[5] a) A. Sánchez-Ferrer, J. N, Rodríguez-López, F, García-Cánovas, F. García-Carmona, *Biochim Biophys Acta.* **1995**, *1247*, 1.; b) M. Sugumaran, *Pigment Cell Res.* **2002**, *15*, 2.; c) M. Sugumaran, *Int. J. Mol. Sci.* **2016**, *17*, 1576.

[6] a) X. Lai, H. J. Wichers, M. Soler-Lopez, B. W. Dijkstra, *Chem. Eur. J.* **2018**, *24*, 47–55.; b) M. Brenner, V. J. Hearing, *Photochem. Photobiol.* **2008**, *84*, 539–549.

[7] R. A- Spritz, J. Oh, K. Fukai, S. A. Homes, L. Ho, D. Chitayat, T. D. France, M. A. Musarella, S. J. Orlow, R. E. Schnur, R. G. Weleber, A. V. Levin, *Human Mutat.* **1997**, *10*, 171.; b) M. Greaves, *Proc. R. Soc. B.* **2013**, *281*,2955.; c) J.-S. Taylor *Science* **2015**, *347*, 824.

[8] a) C. A. Ramsden, P. A. Riley, *Biorg. Med. Chem.* **2014**, *12*, 2388.; b) A. Gibbons, *Science* **2014**, *346*, 934.

[9] a) C. J. Coates, J. Nairn, *Dev. Comp. Immunol.* **2014**, *38*, 43–55.; b) L. Cerenius, K. Söderhäll, *Immunol. Rev.* **2004**, *198*, 116–126.

[10] Y. Matoba, T. Kumagai, A. Yamamoto, H. Yoshitsu, M. Sugiyama, *J. Biol. Chem.* **2006**, *281*, 8981–8990.

[11] C. Kaintz, S. G. Mauracher, A. Rompel. *Advances in Protein Chemistry and Structural Biology* **2014**, *97*, 1-35.

[12] a) M. Kanteev, M. Goldfeder, A. Fishman, *Protein Science* **2015**, *24*, 1360.; b) F. Zekiri, C. Molitor, S. G. Mauracher, C. Michael, R. L. Mayer, C. Gerner, A. Rompel, *Phytochemistry* **2014**, *101*, 5.; c) P. Fronk, H. Hartmann, M. Bauer, E. Solem, E. Jaenicke, S. Tenzer, H. Decker, *Food Chem*. **2015**, *183*, 49.; d) I. Kampatsikas, A. Bijelic, M. Pretzler, A. Rompel, *Sci Rep.* **2017**, *7*, 8860.

[13] a) E. Solem, F. Tuczek, H. Decker, *Angew. Chem. Int. Ed.* **2016**, *55*, 2884–2888; *Angew. Chem.* **2016**, *128*, 2934–2938.; b) H. Decker, E. Solem, F. Tuczek, *Inorg. Chim. Acta* **2018**, *481*, 32–37.

[14] a) E. I. Solomon, D. E. Heppner, E. M. Johnston, J. W. Ginsbach, J. Cirera, M. Qayyum, M. T. Kieber-Emmons, C. H. Kjaergaard, R. G. Hadt, L. Tian, *Chem. Rev.* **2014**, *114*, 3659–3853; b) C. E. Elwell, N. L. Gagnon, B. D. Neisen, D. Dhar, A. D. Spaeth, G. M. Yee, W. B. Tolman, *Chem. Rev.* **2017**, *117*, 2059–2107.; c) E. I. Solomon, U. M. Sundaram, T. E. Machonkin, *Chem. Rev.* **1996**, *96*, 2563–2606.

[15] M. Rolff, J. Schottenheim, H. Decker, F. Tuczek, *Chem. Soc. Rev.* **2011**, *40*, 4077–4098.

[16] M. Réglier, C. Jorand, B. Wagell, *J. Chem. Soc., Chem. Commun.* **1990**, 1752–1755.

[17] a) L. Casella, M. Gullotti, R. Radelli, P. Di Gennaro, *J. Chem. Soc., Chem. Commun.* **1991**, *22*, 1611–1612.; b) L. Santagostini, M. Gullotti, E. Monzani, L. Casella, R. Dillinger, F. Tuczek, *Chem. Eur. J.* **2000**, *6*, 519–522.

[18] a) L. M. Mirica, M. Vance, D. J. Rudd, B. Hedman, K. O. Hodgson, E. I. Solomon, T. D. P. Stack, *Science* **2005**, *308*, 1890–1892.; b) L.

M. Mirica, D. J. Rudd, M. A. Vance, E. I. Solomon, K. O. Hodgson, B. Hedman, T. D. P. Stack, *J. Am. Chem. Soc.* **2006**, *128* (8), 2654.
[19] a) K. V. N. Esguerra, Y. Fall, L. Petitjean, J. P. Lumb, *J. Am. Chem. Soc.* **2014**, *136*, 7662.; b) K. V. N. Esguerra, Y. Fall, J. P. Lumb, *Angew. Chem. Int. Ed.* **2014**, *53*, 5877.; c) M. S. Askari, K. V. N. Esguerra, J. P. Lumb, X. Ottenwaelder, *Inorg. Chem.* **2015**, *54*, 8665.
[20] a) A. Hoffmann, C. Citek, S. Binder, A. Goos, M. Rübhausen, O. Troeppner, I. Ivanović-Burmazović, E. C. Wasinger, T. D. P. Stack, S. Herres-Pawlis, *Angew. Chem. Int. Ed.* **2013**, *52*, 5398-5401; *Angew. Chem.* **2013**, *125*, 5508.; b) P. Liebhäuser, K. Keisers, A. Hoffmann, T. Schnappinger, I. Sommer, A. Thoma, C. Wilfer, R. Schoch, K. Stehrenberg, M. Bauer, M. Dürr, I. Ivanović-Burmazović, S. Herres-Pawlis, *Chem. Eur. J.* **2017**, *23*, 12171.; c) C. Wilfer, P. Liebhäuser, A. Hoffmann, H. Erdmann, O. Grossmann, L. Runtsch, E. Paffenholz, R. Schepper, R. Dick, M. Bauer, M. Dürr, I. Ivanović-Burmazović, S. Herres-Pawlis, *Chem. Eur. J.* **2015**, *21*, 17639.
[21] a) E. L. Presti, E. Monzani, L. Santagostini, L. Casella, *Inorg. Chim. Acta* **2018**, *481*, 47–55.; b) G. Battaini, M. De Carolis, E. Monzani, F. Tuczek, L. Casella, *Chem. Commun.* **2003**, *6*, 726-727.
[22] a) I. Garcia-Bosch, R. E. Cowley, D. E. Dìaz, M. A. Siegler, W. Nam, E. I. Solomon, K. D. Karlin, *Chem. Eur. J.* **2016**, *22*, 5133.; b) I. Garcia-Bosch, R. E. Cowley, D. E. Díaz, R. L. Peterson, E. I. Solomon, K. D. Karlin, *J. Am. Chem. Soc.* **2017**, *139*, 3186.
[23] a) M. Rolff, J. Schottenheim, G. Peters, F. Tuczek, *Angew. Chem. Int. Ed.* **2010**, *49*, 6438.; b) J. N. Hamann, B. Herzigkeit, R. Jurgeleit, F. Tuczek, *Coord. Chem. Rev.* **2017**, *334*, 54.
[24] B. Herzigkeit, B. M. Flöser, N. E. Meißner, T. A. Engesser, F. Tuczek, *ChemCatChem* **2018**, *10*, 5402–5405.
[25] M. S. Askari, L. A. Rodríguez-Solano, A. Proppe, B. McAllister, J.-P. Lumb, X. Ottenwaelder, *Dalton Trans.* **2015**, *44*, 12094–12097.
[26] B. Herzigkeit, B. M. Flöser, T. A. Engesser, C. Näther, F. Tuczek, *Eur. J. Inorg. Chem.* **2018**, *26*, 3058–3069.
[27] a) J. N. Hamann, R. Schneider, F. Tuczek, *J. Coord. Chem.* **2015**, *68*, 3259.; b) J. N. Hamann, F. Tuczek, *Chem. Commun.* **2014**, *50*, 2298–2300.
[28] C. Li, Y. Lien, J. Vinayagam, A. Datta, T. Hua, C. Lin, J. Huang, *Inorg. Chim. Acta* **2015**, *435*, 327–334.
[29] I. Banerjee, J. Marek, R. Herchel, M. Ali, *Polyhedron* **2010**, *29*, 1201-1208.
[30] J. C. Jeffrey, T. B. Rauchfuss, *Inorg. Chem.* **1979**, *18*, 2658–2666.; b) R. Lindner, B. van den Bosch, M. Lutz, J. N. H. Reek, J. I. van der Vlugt, *Organometallics* **2011**, *30* (3), 499–510.; c) J. J. Schneider, *Nachr. Chem.* **2000**, *48*, 614–620.
[31] A. S. Potapov, G. A. Domina, A. I. Khlebnikov, V. D. Ogorodnikov, *Eur. J. Org. Chem.* **2007**, *30*, 5112–5116.
[32] T. Harit, M. Cherfi, J. Isaad, A. Riahi, F. Malek, *Tetrahedron* **2012**, *68*, 4037–4041.
[33] E. Kim, H. Y. Woo, S. Kim, H. Lee, D. Kim, H. Lee, *Polyhedron* **2012**, *42*, 135–141.
[34] a) I. Dvoretzky, G. H. Richter, *J. Org. Chem.* **1950**, *15*, 1285.; b) W. L. Driessen, *Recl. Trav. Chim. Pays-Bas* **1982**, *101*, 441–443.
[35] Y. C. M. Pennings, W. L. Driessen, J. Reedijk, *Polyhedron* **1988**, *7* (24), 2283–2589.
[36] J. R. Cubanski, S. A. Cameron, J. D. Crowley, A. G. Blackman, *Dalton Trans.* **2013**, *42*, 2174.
[37] J. E. Bulkowski, *United States Patent* 4.545.937 **1985**, Oct. 8.
[38] T. Hoppe, P. Josephs, N. Kempf, C. Wölper, S. Schindler, A. Neuba, G. Henkel, *Z. Anorg. Allg. Chem.* **2013**, *639*, 1504–1511.
[39] a) G. Battaini, L. Casella, M. Gullotti, E. Monzani, G. Nardin, A. Perotti, L. Randaccio, L. Santagostini, F. W. Heinemann, S. Schindler, *Eur. J. Inorg. Chem.* **2003**, *6*, 1197–1205.; b) L. Casella, E. Monzani, M. Gullotti, D. Cavagnino, G. Cerina, L. Santagostini, R. Ugo, *Inorg. Chem.* **1996**, *35* (26), 7516–7525.
[40] a) T. N. Sorrell, M. R. Malachowski, *Inorg. Chem.* **1983**, *22* (13), 1883–1887.; b) T. N. Sorrell, A. S. Borovik, D. S. Caswell, C. Grygon, T. G. Spiro, *J. Am. Chem. Soc.* **1986**, *108* (18), 5636–5637.; c) T. N. Sorrell, M. R. Malachowski, D. L. Jameson, *Inorg. Chem.* **1982**, *21*, 3250-3252.
[41] E. I. Solomon, J. W. Ginsbach, D. E. Heppner, M. T. Kieber-Emmons, C. H. Kjaergaard, P. J. Smeets, L. Tian, J. S. Woertink, *Faraday Discuss.* **2011**, *148*, 11–39.

WILEY-VCH

Entry for the Table of Contents

Layout 2:

FULL PAPER

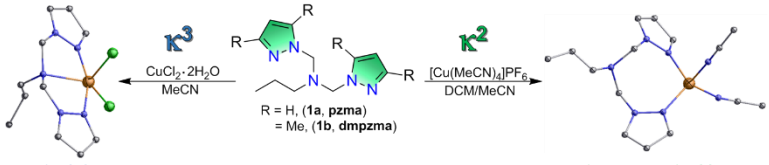

κ² for reactivity. Copper(I) and copper(II) complexes supported by a hemilabile bis(pyrazolylmethyl)amine (**pzma**) ligand have been synthesized and structurally characterized. The corresponding copper(I) complexes were used as catalysts for the tyrosinase-like oxygenation of 2,4-di-*tert*-butylphenol (DTBP-H).

Copper Tyrosinase Models

*Benjamin Herzigkeit, Ramona Jurgeleit, Benedikt M. Flöser, Nadja E. Meißner, Tobias A. Engesser, Christian Näther, Felix Tuczek**

Page No. – Page No.

Employing linear tridentate ligands with pyrazole endgroups in catalytic tyrosinase model chemistry: Does hemilability matter?